Fuel 278 (2020) 118269

Contents lists available at ScienceDirect

Fuel

journal homepage: www.elsevier.com/locate/fuel

Full Length Article

Gaseous emissions (regulated and unregulated) and particulate characteristics of a medium-duty CRDI transportation diesel engine fueled with diesel-alcohol blends

Vikram Kumar, Akhilendra Pratap Singh, Avinash Kumar Agarwal*

Engine Research Laboratory, Department of Mechanical Engineering, Indian Institute of Technology Kanpur, Kanpur 208016, India

ARTICLE INFO

Keywords:
Diesel
Alcohols
Diesohols
Particulate matter
Unregulated emissions

ABSTRACT

In this study, different diesel-alcohol (methanol, ethanol, and butanol) blends termed as 'diesohols' were used to investigate the performance and emission characteristics of a modern common rail direct injection (CRDI) transportation diesel engine. A comparative characterization of regulated emissions, unregulated emissions, and particulate matter (PM) to explore suitability of methanol, ethanol, and butanol blending with mineral diesel was the main objective of this study. In this study, engine experiments were performed at different engine loads (3, 6, 9 and 12 bar BMEP) and speeds (1500, 2500 and 3500 rpm). Results showed that the use of diesohols improved the engine performance, leading to relatively higher brake thermal efficiency (BTE) compared to baseline mineral diesel. Addition of alcohols in mineral diesel reduced both, the PM, and the oxides of nitrogen (NOx) emissions and this reduction was dominant at higher engine loads. Trace concentrations of various unregulated emission species such as isocyanic acid (HNCO), formaldehyde, etc. increased slightly with addition of alcohols in baseline mineral diesel. However, diesohol-fueled engine emitted relatively lower concentrations of sulfur dioxide (SO_2), nitrogen oxide (NO), etc. compared to baseline mineral diesel. Amongst different primary alcohols, methanol showed most significant reduction in NOx and PM emissions and most significant increase in BTE compared to other alcohols. Overall, addition of alcohol, especially methanol and ethanol in mineral diesel showed significant potential for engine performance improvement and exhaust emission reduction in a medium-duty CRDI transportation diesel engine.

1. Introduction

Diesel engines are widely used in various sectors of economy due to their higher efficiency, durability, and reliability compared to their spark-ignited (SI) gasoline engine counterparts. However in the last few decades, mineral diesel-fueled compression ignition (CI) engines are criticized heavily for producing environmental pollution and fossil fuel consumption. Oxides of nitrogen (NOx) and particulate matter (PM) emitted from diesel engines are harmful to the human health and potentially cause respiratory diseases. In many studies, PM has been reported to be the main source of mutagenicity and carcinogenicity in the engine exhaust [1]. PM originating from CI engines comprise of highly agglomerated solid carbonaceous matter and volatile organic compounds (VOCs), vaporized/pyrolyzed fuel, lubricating oil, trace metals, and sulfates [2]. Solid carbonaceous core or the soot in the PM mainly originates from the unburnt fuel, which nucleates from vapor-phase to solid-phase in fuel-rich regions of the combustion chamber at elevated temperatures, typically in the diffusion flames [3–4]. Many researchers have suggested that the PM formation takes place in several stages, starting with combustion of non-homogeneous fuel–air mixture, which can be reduced by many techniques including use of optimized fuel injection parameters, and oxygenated alternative fuels [5–7].

On the other hand, increasing energy demands and limited resources of fossil fuels have opened up new opportunities for large-scale utilization of alternative fuels such as primary alcohols, which are relatively lower cost, renewable and cleaner fuels compared to conventional fossil fuels used in transport sector such as petrol and mineral diesel [8–9]. These primary alcohols such as methanol, ethanol, and butanol can be used as fuel in diesel engines, with potential of reduction in emissions of harmful pollutants. Fuel properties of alcohols improve the spray characteristics of diesohols and additional fuel-bound oxygen present in alcohols results in more complete combustion [10–12]. Presence of oxygen in alcohol molecules alters their oxidation pathways. Oxygen improves the oxidation of fuel carbon atoms, leading to

* Corresponding author.
E-mail address: akag@iitk.ac.in (A.K. Agarwal).

https://doi.org/10.1016/j.fuel.2020.118269
Received 23 April 2020; Received in revised form 26 May 2020; Accepted 28 May 2020
Available online 07 June 2020
0016-2361/

relatively reduced participation of carbon in growth pathways, which reduces the formation of higher molecular weight compounds [13]. During fuel-rich combustion conditions (global or local) in the combustion chamber, partial oxidation might occur leading to formation of oxygenated species with high molecular weight, which reduces PM formation as well as its growth [14–16]. The main challenge of using primary alcohols in existing diesel engines include its lower cetane number and higher corrosiveness [17]. A number of methods can be used for alcohol utilization in diesel engines including fumigation [18], dual-fuel injection [19], blending and emulsification [20–24]. Among these methods, blending of primary alcohols with mineral diesel is the simplest and most adapted technique for alcohol utilization in diesel engines. However, this technique cannot be used in higher blending ratios, especially for Methanol, due to its miscibility issues with mineral diesel. Hence only lower diesohol blends are used in diesel engines mostly. Few researchers have explored the use of additives to improve the miscibility of primary alcohols with mineral diesel for achieving higher diesohol blends with limited success [25]. To investigate diesohol blend stability and their potential, researchers have investigated the performance, combustion and gaseous and PM emissions from diesel engines fueled with diesohols (methanol, ethanol, and butanol blended with diesel) [26–27]. Canakci et al. [28] investigated engine combustion, performance, and emissions characteristics of a single-cylinder, four-stroke diesel engine fueled with blends of diesel/methanol (0–15% v/v). Increasing methanol fraction in the test fuel results in increased brake specific fuel consumption (BSFC) and NOx emissions, and reduced hydrocarbon (HC) and carbon monoxide (CO) emissions. Agarwal et al. [25] performed a similar study, in which a single-cylinder diesel engine was fueled with diesel/methanol blends (10 and 15% v/v). They reported that the addition of methanol in mineral diesel improved engine performance and reduced emissions. Higher blending ratio of methanol in mineral diesel resulted in lower NOx emissions compared to baseline mineral diesel. Huang et al. [29] focused on the oxygen content of diesel/methanol blends (0 to 14% w/w). They found that increasing oxygen percentage in the test fuel shifted the combustion predominantly towards the premixed combustion phase, which reduced the emissions of CO and smoke but increased NOx emissions slightly.

Very few researchers investigated unregulated emissions from the use of diesohols in diesel engines [30–32]. Agarwal et al. [30] investigated unregulated emissions from a CI engine fueled with 5% methanol blended diesel (MD5) and reported no significant change in unregulated emissions compared to baseline mineral diesel. A detailed study of unregulated emissions (CH_3CHO, HCHO, and NO_2) was done by Zhou and Qiu [31] using a six-cylinder, turbocharged, CRDI diesel engine employing dual fuel technique for utilization of diesel and alcohols. Alcohol was injected into the intake manifold and diesel was directly injected into the engine combustion chamber using CRDI system. They reported that introduction of alcohol as secondary fuel in diesel engine resulted in higher emissions of unregulated species, which further increased with increasing premixed ratio of methanol. They suggested that unregulated emissions can be controlled by using exhaust gas after-treatment devices such as diesel oxidation catalysts (DOC). Sayin [33] studied the performance and emission characteristics of a CI engine by using diesel-methanol and diesel-ethanol blends (5% and 10% v/v). Addition of alcohols with mineral diesel increased the NOx emissions and BSFC, and reduced the brake thermal efficiency (BTE), HC, and CO emissions as well as smoke opacity. Jamrozik [34] investigated the effect of higher diesohol blends (ethanol and methanol up to 40% v/v) on engine performance and emission characteristics of a direct injection single-cylinder engine. They reported that increasing blending ratio resulted in higher BTE and CO emission, however CO_2 and HC emissions remained unchanged. Merritt et al. [35] investigated regulated and unregulated emissions from a heavy-duty diesel engine fueled with ethanol-diesel blends. They reported that increasing blending ratio of ethanol in mineral diesel resulted in reduced PM emissions, reduced smoke opacity, reduced emissions of organic compounds such as 1, 3-Butadiene, 1-nitropyrene, polycyclic aromatic hydrocarbons (PAHs), and Benzene but increased emission of acetaldehyde. He et al. [36] also investigated the effect of blending ratio of ethanol in mineral diesel, and reported that smoke opacity, emissions of NOx and CO_2 reduced, however emissions of ethanol, acetaldehyde, and CO increased with increasing blending ratio. They also reported that use of an ignition improver additive reduced the emissions of unburned ethanol, CO and acetaldehyde. Cheung et al. [37] also performed experiments to investigate regulated and unregulated emissions from a direct injection diesel engine fueled with diesel-ethanol blends. They reported that addition of ethanol in mineral diesel reduced emissions of CO and HC at high engine loads, however, NOx reduction potential was limited up to low engine loads only. Ethanol blending with mineral diesel was helpful in reducing emissions of ethane, formaldehyde, 1,3-butadiene, ethylene, benzene, toluene, and xylene at higher engine loads, however, emission of acetaldehyde increased. Presence of ethanol in diesohol showed a remarkable effect on PM emissions, which reduced significantly at high engine loads. Lapuerta et al. [38] used a Euro-VI engine for evaluating the effect of butanol addition (up to 20% v/v) in mineral diesel. They reported that diesel-butanol blend-fueled engine emitted relatively higher CO and HC emissions compared to baseline mineral diesel. They concluded that diesohol with butanol (up to 16% v/v) was the optimum blend ratio, which reduced the PM emissions significantly compared to baseline mineral diesel. Further higher blending ratios led to negative results of PM reduction. Chen et al. [39] investigated the performance and emissions characteristics of a direct injection diesel engine using diesel-butanol blends (up to 40% v/v). The results showed that addition of butanol resulted in increasing BTE. Butanol-diesel blends were effective for NOx reduction up to low loads only and at higher engine loads, NOx emissions increased with increasing blending ratio of butanol. Smoke opacity decreased with increasing butanol blending ratio. Choi and Jiang [40] investigated HC and PM emissions emanating from a turbocharged diesel engine fueled with diesel-butanol (5, 10, and 20% v/v) blends at various loads and speeds. They reported that benzene, ethylene, and formaldehyde emissions were higher at low loads, which increased with increasing butanol blending ratio. They also measured the number-size distribution of particles emitted by diesel-butanol blend-fueled engine and reported that butanol blending with mineral diesel resulted in emission of higher number of particles of relatively smaller size compared to baseline mineral diesel. Yusri et al. [41] investigated the combustion and emission characteristics of a diesel engine fueled with diesel-butanol (5, 10, and 15 v/v) blends. They reported that butanol addition with mineral diesel resulted in relatively lower emissions of CO, HC and NOx compared to baseline mineral diesel. Kim et al. [42] performed experiments using diesel-butanol blends and reported similar trends. Liu et al. [43] investigated the effect of blending ratio on particulate emission characteristics of diesel-butanol blend fueled partially premixed combustion (PPC) engine. They reported that increasing blend ratio of butanol resulted in lower number concentration of accumulation mode particles (AMP), however number concentration of the nucleation mode particles (NMP) increased sharply. Total number and mass concentration of particulates reduced with increasing blend ratio of butanol in the test fuel.

The literature discussed above clearly shows the potential of primary alcohols (methanol, ethanol, and butanol) for the partial displacement of mineral diesel in modern CI engines used in transport sector. Different fuel injection strategies and their effects are discussed earlier in this paper. It is clear that only lower diesohol blends (up to 10% v/v) are suitable to be implemented at a large-scale and diesohol blends with higher blending ratio (> 10% v/v) remain of academic interest only. Most studies carried out using diesohol blends focused on engine's combustion, performance and emissions characteristics. Very few studies are reported, which investigated unregulated emission and particulate characteristics of modern CRDI transportation diesel

Table 1
Technical specifications of the test engine and dynamometer.

Engine Make/ Model	Tata/ Safari DICOR 3.0 L
Engine Type	Water-cooled, Turbo-charged, Inter-cooled
Bore/ Stroke	97/ 100 mm
Number of Cylinders	Four
Cubic Capacity	2956 cc
Rated Power Output	84.5 kW @ 3000 rpm
Rated Torque	300 Nm @ 1800–2000 rpm
Compression Ratio	17.5
Fuel Injection System	CRDI; 1600 bar max fuel injection pressure
Dynamometer Make/ Model	Dynomerk/ EC-300
Type	Eddy Current
Rated Capacity	220 kW @ 2500–8000 rpm
Rated Torque	702 Nm @ 8000 rpm

engines fueled with diesel-alcohol blends. In this study, unregulated emissions and PM characteristics of a medium-duty transportation CRDI engine are explored using three diesohols namely DM10 (10% methanol blended with diesel, v/v), DE10 (10% ethanol blended with diesel, v/v) and DB10 (10% butanol blended with diesel, v/v) vis-a-vis baseline mineral diesel. Experiments were performed at different engine loads (3, 6, 9 and 12 bar BMEP) and speeds (2000, 2500 and 3000 rpm) to cover the entire operating range of the CRDI test engine selected for the purpose. A comprehensive comparative study of suitability of methanol, ethanol, and butanol blending in mineral diesel is the novelty of this study. Detailed characterization of PM emitted from engine fueled with DM10, DE10 and DB10 is another innovative aspect of this study, which has not been reported in the literature previously.

2. Experimental setup and methodology

To investigate the PM and unregulated emission characteristics of different diesohols, a four-cylinder in-line, four-stroke, CRDI transportation CI engine (Tata; Safari DICOR 3.0 L), was chosen as a test engine (Table 1). The engine consisted of a high-pressure fuel pump connected with a common rail, which supplied high-pressure fuel to the electronically controlled solenoid injectors. All control parameters such as fuel injection pressure (FIP), fuel injection timing, fuel quantity, etc. were controlled by an electronic control unit (ECU). This engine was coupled with an eddy current dynamometer (Dynomerk; EC-300) to control the engine speed and load according to the engine operating conditions and requirements of the test. The dynamometer controller displayed the temperature of lubricating oil and coolant, in order to avoid any failure due to excessive heating. During the experiments, temperature of lubricating oil and coolant were maintained at ~ 90 °C and ~ 75 °C respectively. The schematic of the experimental setup is shown in Fig. 1 and the technical specifications of the test engine and dynamometer are given in Table 1.

For engine performance and emission characterisation, intake air-flow rate and fuel consumption rate were measured. For air-flow rate measurement, a laminar flow element (LFE) and a U-tube manometer were used. Pressure difference across the orifice plate was measured using the U-tube manometer. For measurement of the exhaust gas temperature (EGT), a K-type thermocouple with an accuracy of ± 2 °C having a digital display unit was used. To minimize errors in the measurement of EGT, thermocouple was installed very close to the exhaust port, and EGT was measured only after thermal stabilization of the engine at each measurement point. For emission characterization, three emission analyzers were used in this study namely: Raw exhaust gas emissions analyzer (Horiba; EXSA-1500) for regulated gaseous species measurement; Fourier transform infrared (FTIR) emissions analyzer (Horiba; MEXA-6000FT-E) for unregulated species measurements, and engine exhaust particle sizer (EEPS) spectrometer (TSI Inc.; 3090) for particulate characterization. Raw exhaust gas emisison analyzer measured regulated gaseous emission species namely CO, HC, NOx, and CO_2. In this analyzer, non-dispersive infrared (NDIR) technique was employed to measure CO and CO_2 emissions, flame ionization detection (FID) technique was employed to measure HC emissions, and Chemiluminescence (CLD) technique was employed for measuring NOx emissions. FTIR emission analyzer is a combination of an interferometer and a high-speed Fourier transform, which absorbs the high resolution infrared spectrum to measure the unregulated gaseous emission species precisely. Exhaust gas sampling systems of Regulated emission analyzer and FTIR emission analyzer were maintained at 191 °C by using a heated sampling line, as per the US Environmental Protection Agency (USEPA) norms, in order to avoid condensation of high boiling point hydrocarbons and moisture during the sampling. Other details of these emission analyzers can be seen in our previous publications [30,44]. EEPS spectrometer measured the engine exhaust particles in the sizes ranging from 5.6 nm to 560 nm, with a maximum concentration up to $\#10^8$ particles/cm^3 of the exhaust gas. To avoid excessive concentration error at higher engine loads, a rotating disk thermo-diluter (Matter Engineering AG; MD19-2E) was used to dilute the exhaust gas before its entry into the EEPS. Detailed working principle of EEPS can be found in our previous publications [44–45]. Technical specifications of the EEPS are given in Table 2.

For test fuel preparation, a mechanical stirrer (Remi equipment; RQT-124A) was used at 1800 rpm. In this study, blending of different alcohols with mineral diesel was limited only up to 10% (v/v). This was mainly due to miscibility issues of methanol with mineral diesel, which exhibited separation at blending ratios higher than 10% v/v. These blending issues have been reported in many previous studies [25,46] as well. Fig. 2 shows the fuel mixing system used for blending the test fuels and two methanol-diesel blends namely unstable DM15 (15% v/v methanol blended with mineral diesel) and stable DM10 (10% v/v methanol blended with mineral diesel). To ensure no phase separation, all test fuels were stored for 48 h before their use. All test fuels exhibited stable blend characteristics.

Important test fuel properties such as density, kinematic viscosity and calorific value of mineral diesel, DM10, DE10, and DB10 were measured using portable density meter (Kyoto Electronics; DA130N), kinematic viscometer (Stanhope-Seta; 83541–3), and bomb calorimeter (Parr; 6200), respectively. The calorific value of diesohols was relatively lower than baseline mineral diesel, primarily due to relatively lower calorific values of constituent alcohols [10,25]. Important test fuel properties are shown in Table 3.

All measurements were done after thermal stabilization of the engine in order to reduce the experimental errors. To reduce measurement errors, experiments were performed thrice and an average of these measurements was used as raw data for further analysis. In this study, root-of-the-sum-of-the-squares (RSS) method was used for the uncertainty analysis, in which all uncertainties such as precision, bias, calibration and measurement uncertainties were considered.

3. Results and discussion

The results of engine experiments performed using three diesohols and baseline mineral diesel are discussed in three sub-sections namely: (i) performance and regulated emissions, (ii) unregulated emissions, and (iii) PM emissions. In each sub-section, results show (i) the effect of varying engine load (BMEP) from (3, 6, 9, and 12 bar) at constant engine speed (2500 rpm), and (ii) the effect of varying engine speed (2000, 2500 and 3000 rpm) at constant BMEP (6 bar). These engine operating conditions were selected based on the engine's operation 'on-road'. Most times, vehicles operate in this speed range at roughly constant engine load (~50% of full load), while cruising at highways.

3.1. Performance and regulated emissions

In this study, three performance parameters (BTE, brake specific energy consumption (BSEC) and EGT) of a diesohol-fueled engine were

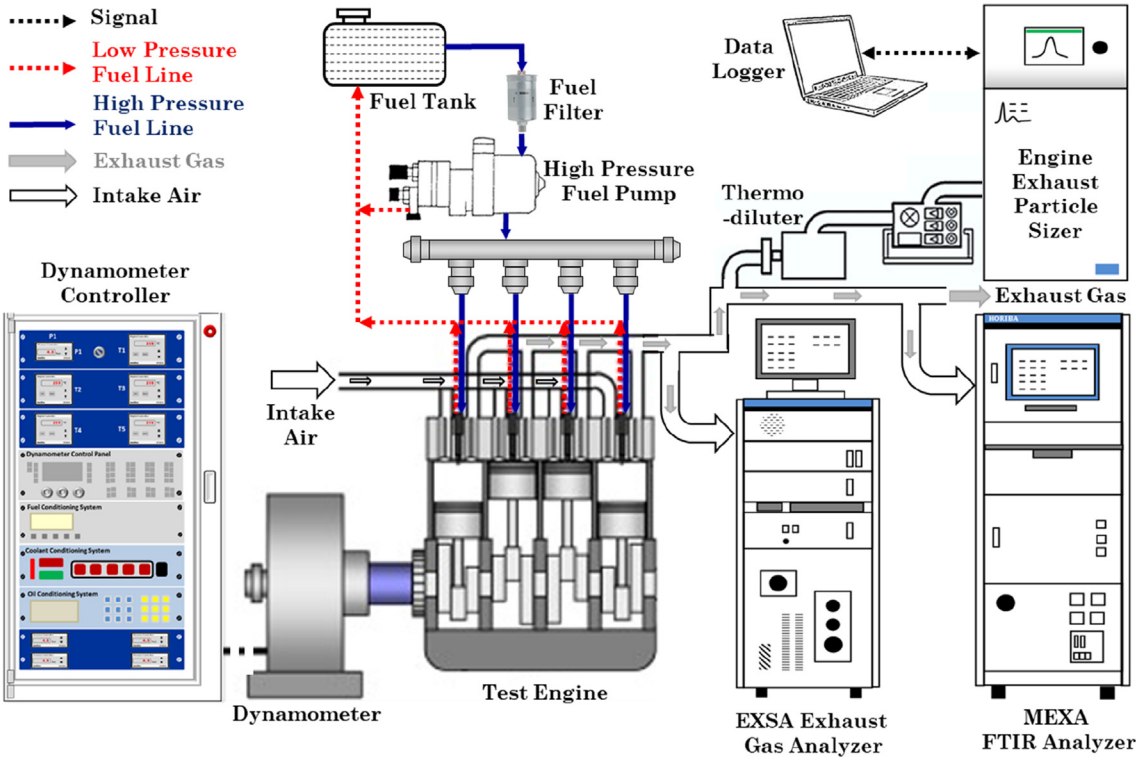

Fig. 1. Schematic of the experimental setup.

Table 2
Technical specifications of the EEPS.

Make/ model	TSI/ EEPS 3090
Particle size range	5.6–560 nm
Electrometer channels	22
Time resolution	10 Hz
Sample flow rate	10 L/min
Operating temperature range	0–40 °C
User interface	EEPS software
Maximum concentration	#10^8 particles/cm^3

compared. These performance parameters were then qualitatively correlated with regulated emissions (CO, HC, and NOx) (Figs. 3 and 4). Raw emissions were measured in ppm, and then converted to mass emissions (in g/kWh) using standard BIS and SAE procedures [47]. The first part of this sub-section presents the variations in engine performance and emission characteristics at varying BMEP (Fig. 3).

Fig. 3 shows the variations in performance and emissions characteristics of engine fueled with diesohols at different engine loads. Results showed that BTE increased with increasing engine load. At a lower BMEP (3 bar), BTE for all diesohols as well as mineral diesel were almost similar and as the engine load increased, the BTE also increased. However, the increments were different for different test fuels. Results showed that blending of primary alcohols with mineral diesel improved engine performance and resulted in higher BTE compared to baseline mineral diesel. The maximum BTE was observed for DM10 at 12 bar BMEP, which was ~ 5% higher than baseline diesel. At 12 bar BMEP, lower BTE of mineral diesel compared to diesohols might be possibly due to the presence of relatively richer fuel–air mixture, leading to

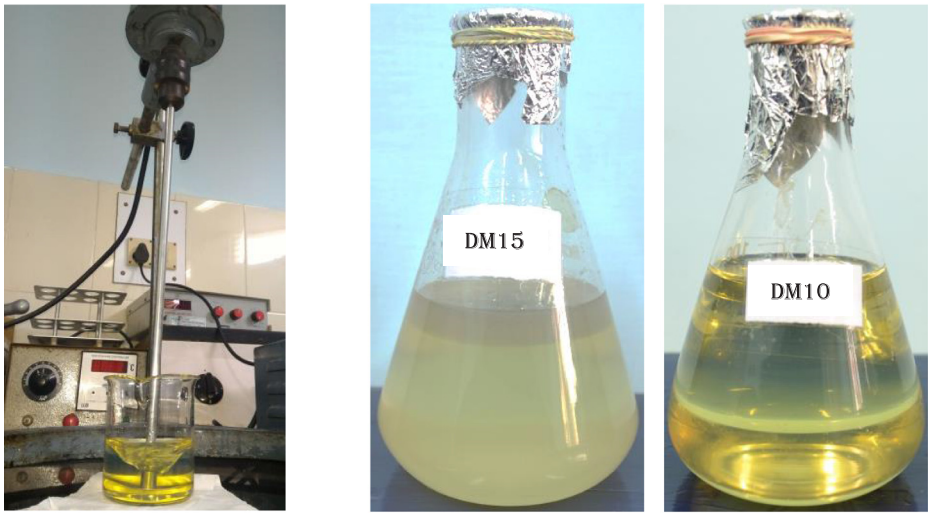

Fig. 2. Blend preparation system, unstable DM15 and stable DM10 fuel blend.

Table 3
Important test fuel properties.

Test fuel	Diesel	DM10	DE10	DB10
Composition	100% diesel	10% v/v methanol, 90% v/v diesel	10% v/v ethanol, 90% v/v diesel	10% v/v butanol, 90% v/v diesel
Calorific Value (MJ/kg)	44.26	40.78	41.33	42.86
Kinematic Viscosity @ 40 °C (mm^2/s)	2.96	2.74	2.82	2.93
Density (g/cm^3) @ 30 °C	0.837	0.819	0.822	0.834

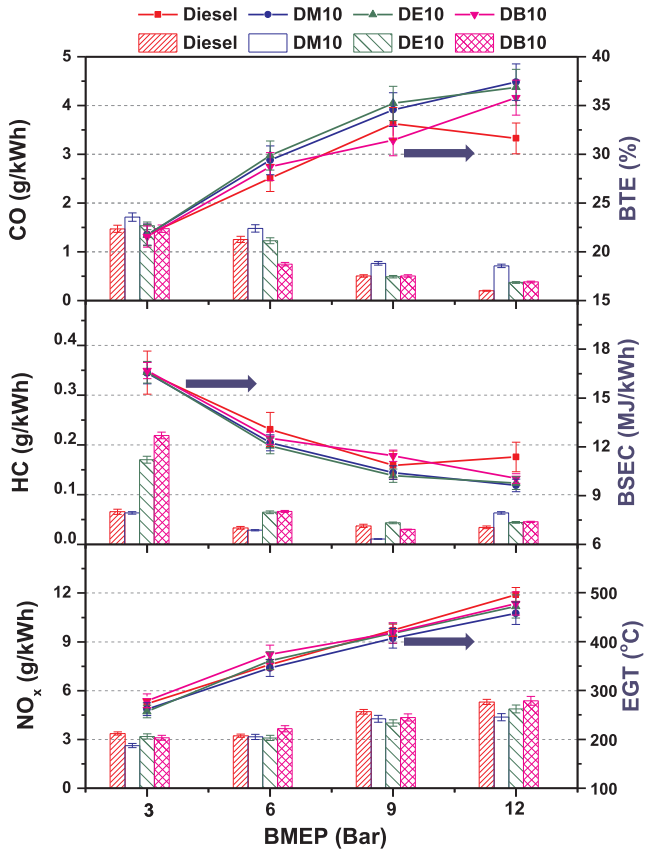

Fig. 3. Performance and regulated emissions variations from diesohols with varying BMEPs at constant engine speed of 2500 rpm.

higher degree of incomplete combustion. Increased heat transfer due to relatively higher EGT of mineral diesel at 12 bar BMEP might be another possible reason for lower BTE [3]. Relatively lower BTEs at higher engine loads were also reported by Lee et al. [48]. Among different diesohols, DM10 exhibited relatively higher BTE compared to DE10 and DB10 (except at 6 bar BMEP). This was mainly due to combined effect of fuel properties of methanol and availability of fuel oxygen (~4.75% w/w), which led to more complete combustion [30,46]. Relatively higher flame-speed of DM10 might be another possible factor, which improved combustion, resulting in higher BTE [46]. Relatively lower peak in-cylinder temperature during the combustion of DM10, which led to lower heat transfer from the cylinder walls might be another potential reason for higher BTE [3,49]. BSEC showed an inverse trend than that of BTE. BSEC at lower BMEP was the highest, which reduced with increasing BMEP. The lowest value of BSEC was ~ 9 MJ/kWh for DM10 at 12 bar BMEP and the highest BSEC was ~ 16 MJ/kWh at 3 bar BMEP. EGT is an indirect measure of bulk in-cylinder temperature. EGT increased with increasing engine load, primarily due to combustion of relatively larger fuel quantity at higher engine loads. Alcohol blending with mineral diesel reduced the EGT at all engine loads. Relatively higher latent heat of vaporization of alcohols was the main factor responsible for this trend. Similar results of EGT variations were also reported in previous studies [23,25,46]. Among different diesohols, DM10 exhibited the lowest EGT due to significantly higher latent heat of vaporization of methanol compared to ethanol and butanol, however EGTs of DE10 and DB10 were almost similar.

Emission results showed that CO and HC emissions decreased with increasing engine load. Both CO and HC are incomplete combustion products, formed due to lower in-cylinder temperatures and oxygen deficiency [3]. At higher engine loads, higher in-cylinder temperature promoted more complete combustion, hence lower HC and CO emissions. Alcohol blending with mineral diesel resulted in slightly higher HC and CO emissions, primarily due to relatively higher latent heat of vaporization of alcohols compared to mineral diesel. Yusri et al. [41] and Kim et al. [42] also reported similar findings. Among different diesohols, DM10 exhibited the highest CO emission and DE10 exhibited the highest HC emissions. Relatively higher CO emission from DM10 was mainly due to higher latent heat of vaporization of methanol compared to other alcohols, which resulted in relatively lower in-cylinder temperature. This was also seen in the EGT trends (Fig. 3). Agarwal et al. [25] and Singh et al. [46] also reported similar trends. NOx emissions increased with increasing engine load. NOx emissions are mainly affected by the peak in-cylinder temperature, localized oxygen availability and reaction time [3]. Increasing engine load results in higher in-cylinder temperature, and hence more NOx formation takes place. Alcohol blending with mineral diesel reduced NOx emissions due to reduction in the peak in-cylinder temperature. This trend was also observed for EGT, which exhibited a qualitative measure of peak in-cylinder temperature [23,42]. Relatively higher latent heat of vaporization of alcohols compared to mineral diesel was the main reason of relatively lower peak in-cylinder temperature of diesohols. Among different diesohols, DM10 emitted the lowest NOx, followed by DE10, and DB10.

The second part of this sub-section presents the variations in the engine performance and emission characteristics at different engine speeds (2000, 2500, and 3000 rpm) (Fig. 4). Fig. 4 shows that BTE decreased with increasing engine speed at constant engine load. Incomplete combustion due to lesser time available at higher engine speeds was the main reason for this trend. Alcohol blending with mineral diesel resulted in slightly higher BTE, which was more dominant for methanol and ethanol. At all engine speeds, DM10 and DE10 resulted in relatively higher BTE compared to mineral diesel and DB10. Among different test fuels, DM10 exhibited the lowest BSEC. EGT increased with increasing engine speed. Among different diesohols, DM10 exhibited the lowest EGT, which was dominant at 3000 rpm.

Fig. 4 also showed the emission characteristics of all test fuels at varying engine speeds at fixed BMEP. Results showed that CO and HC emissions from mineral diesel-fueled engine first increased and then decreased. Alcohol blending in mineral diesel resulted in slightly higher HC and CO emissions compared to mineral diesel (except CO emission at 2500 rpm). At 2500 rpm, reduction in chemical kinetics of fuel–air mixture due to alcohol blending in mineral diesel may be a possible reason for this trend, which became dominant at 2500 rpm, resulting in higher variations in CO emission from different test fuels. At 2500 rpm, a trade-off between increased turbulence and available time for heat transfer from the cylinder walls might be another possible reason, leading to increased heat transfer. This might have led to relatively lower in-cylinder temperature, hence higher CO emission. Relatively

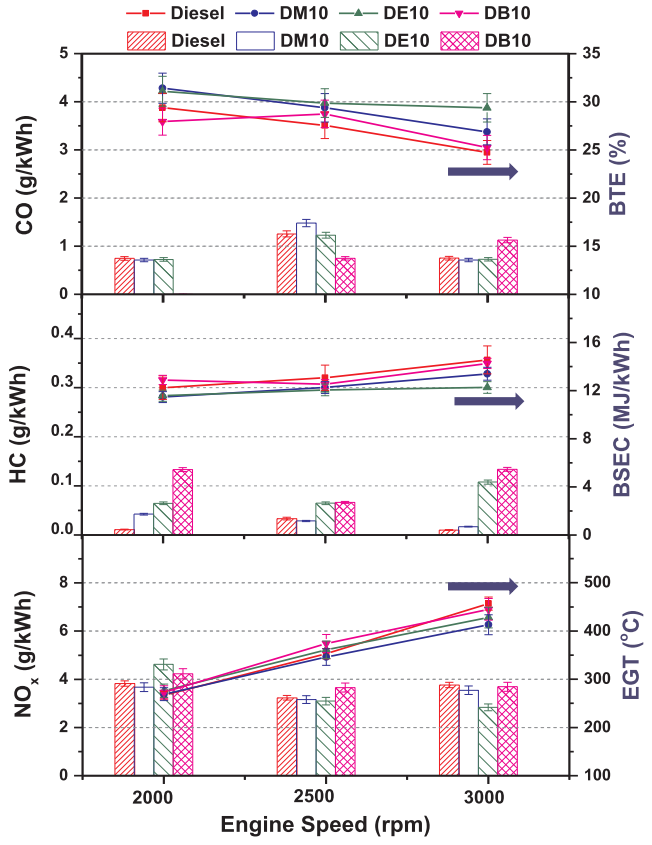

Fig. 4. Performance and regulated emissions variations for diesohols with varying engine speeds at constant BMEP of 6 bar.

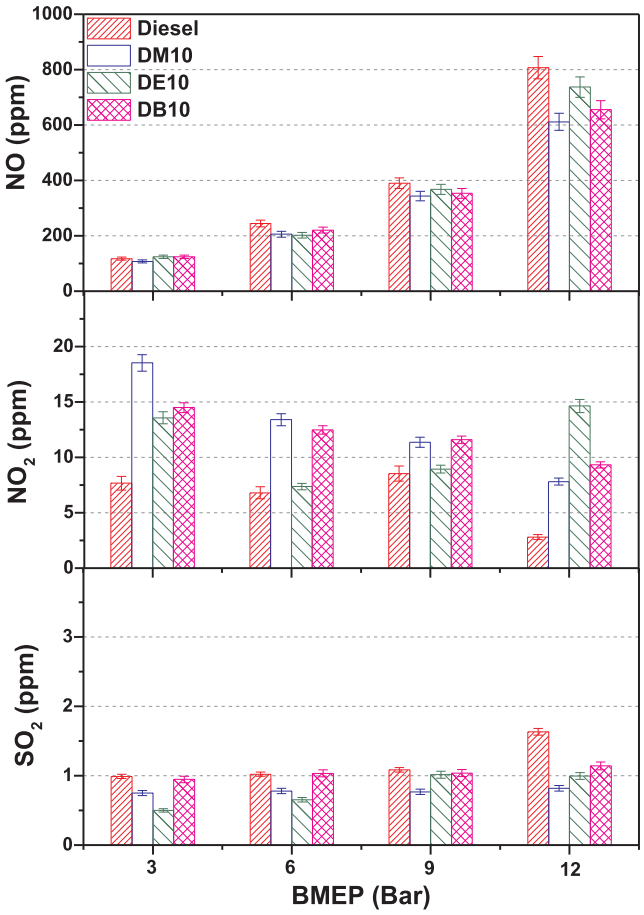

Fig. 5. Unregulated emission (inorganic species) characteristics of diesohols with varying BMEPs at constant engine speed of 2500 rpm.

higher HC emissions from DB10-fuelled engine was an important observation of this study. This might be due to combined effect of relatively higher latent heat of vaporization compared to mineral diesel, and lower flame-speed compared to other diesohols, which might have resulted in higher degree of incomplete combustion of fuel near the cylinder walls [23,42]. Kim et al. [42] also carried out engine experiments using mineral diesel blended with hydrated butanol and reported similar observations. NOx emissions at different engine speeds showed an important trend. Although EGT increased with increasing engine speed, however NOx emissions reduced slightly. This was mainly due to two effects (i) shifting to predominantly diffusion combustion phase due to less time availability for fuel–air premixing, and (ii) less time availability for NOx formation. Effect of relatively lower in-cylinder temperature at 2500 rpm was also visible in NOx emissions. Results showed that DM10 emitted the lowest NOx emissions at different engine speeds, possibly due to charge cooling effect of methanol blended with mineral diesel.

3.2. Unregulated emissions

Figs. 5 and 6 show the unregulated emission characteristics of DM10, DE10, DB10 and mineral diesel-fueled engine at varying engine speeds and loads. These unregulated gaseous species were measured using FTIR emission analyzer, which was capable of measuring 31 unregulated emission species precisely [25,44]. However, only six species were detected in this study with reasonable confidence and precision and remaining unregulated emission species (ammonia, formaldehyde, formic acid, methane, ethylene, ethane, propylene, propane, 1,3-butadine, acetic acid, acetylene, ethanol, acetaldehyde, methanol, *iso*-pentane, n-pentane, n-octane, *iso*-butylene, n-butane, isobutene, benzene, toluene) were below the detection limit of the instrument. The detected unregulated species are divided into two categories namely (i) inorganic species (such as NO, NO_2 and SO_2), and (ii) carbonyl species (such as HCHO, HCOOH, and HNCO). These species have been grouped based on their concentration levels in the exhaust. The first part of this sub-section presents the variations in unregulated emission (inorganic species) characteristics at varying BMEP (Fig. 5) at constant engine speed of 2500 rpm. The second part of this sub-section presents the variations in unregulated emission (inorganic species) characteristics at varying engine speeds (Fig. 6) at constant BMEP of 6 bar.

Results showed that increasing BMEP resulted in higher NO emission for all test fuels, mainly due to higher fuel quantity being injected into the combustion chamber. This resulted in higher peak in-cylinder temperature, which created favorable conditions for NO formation. Relatively lower NO emission from diesohols compared to baseline mineral diesel was an important observation. This trend was noticeable dominantly at higher BMEP, where the charge cooling effect of alcohols was significant. Among different diesohols, DM10 exihibited the highest reduction in NO emission. This is directly correlated to distinct methanol property of the highest latent heat of vaporization amongst all test alcohols.

NO_2 emission followed an exactly opposite trend than NO emission and it decreased slightly with increasing engine load. NO_2 formation is governed more by localized oxygen availability, which reduced at higher BMEPs. Relatively higher NO_2 emissions from diesohols compared to baseline mineral diesel was an important observation. In NO_2 variations, a weak correlation with fuel oxygen was also observed. As the fuel oxygen increased, NO_2 emission also increased e.g. DM10 resulted in the maximum NO_2 emissions up to 9 bar BMEP. However, as an experimental outlier, DE10 emitted the maximum NO_2 at 12 bar

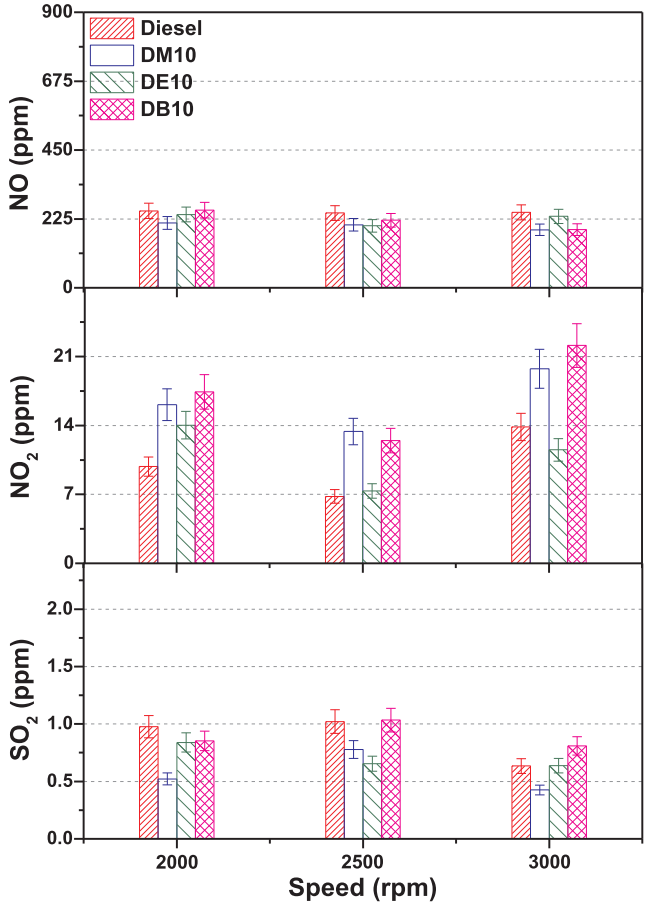

Fig. 6. Unregulated emission (inorganic species) characteristics of diesohols with varying engine speeds at constant BMEP of 6 bar.

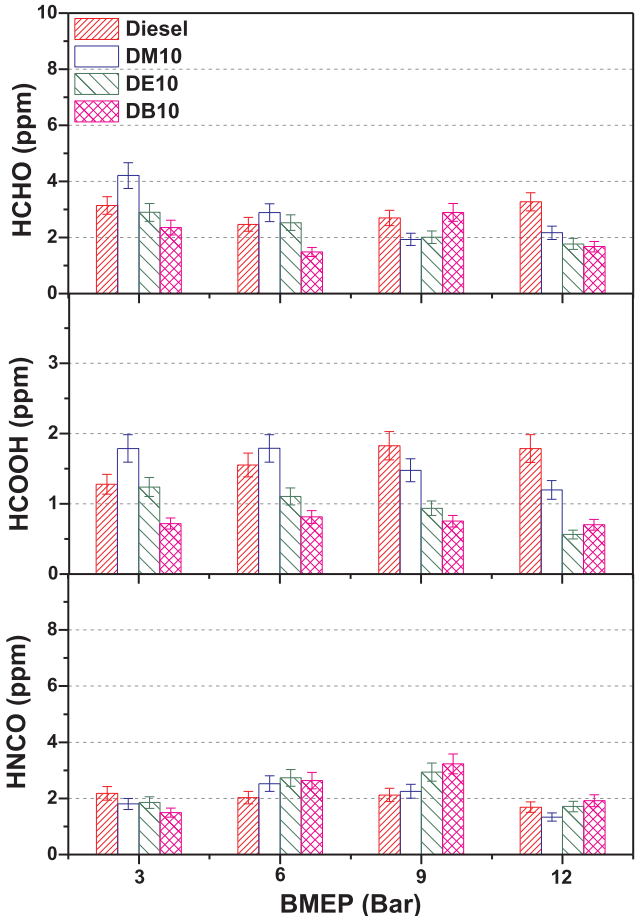

Fig. 7. Unregulated emission (carbonyl species) characteristics of diesohols with varying BMEPs at constant engine speed of 2500 rpm.

BMEP. SO_2 emitted by diesel engine is yet another important unregulated species, which mainly originates from fuel sulfur. Fig. 5 shows very low levels of SO_2 emission from diesohol-fueled engine, which was marginally lower than baseline mineral diesel. With increasing engine load, SO_2 emitted from the engine remained almost constant for all test fuels. This might be due to the fact that 90% of the fuel constituent in all test fuels was still mineral diesel and SO_2 from mineral diesel participated in PM formation, as a soot precursor. A fraction of SO_2 produced in the combustion chamber also gets converted into H_2SO_4 after reacting with water vapors and gets adsorbed on to the particle surface. Presence of H_2SO_4 vapors in the exhaust acts as a site for condensation of volatile materials, which promotes soot formation with higher adsorbed organic content.

Fig. 6 shows that NO emission from all test fuels were almost identical at different engine speeds. At maximum engine speed, NO emission reduced slightly, possibly due to availability of lesser time for NO formation. Among different diesohols, DM10 exhibited the lowest NO emission.

For all test fuels, increasing engine speed first reduced and then increased the NO_2 emission and was the lowest at 2500 rpm. Among all diesohols, DB10 emitted the highest NO_2, followed by DM10. With increasing engine speed, SO_2 emission remained almost constant up to 2500 rpm, however, it reduced slightly at 3000 rpm, although the values were very low. DM10 and DE10 emitted slightly lower SO_2 compared to baseline mineral diesel, and DB10 emitted almost similar SO_2 as that of baseline mineral diesel.

Figs. 7 and 8 showed variations of carbonyl species emitted from diesohols and mineral diesel-fueled engine at different engine loads and speeds, respectively. The term 'carbonyl' refers to the carbonyl functional group, which is a bivalent group consisting of a carbon atom double-bonded to oxygen. The carbonyls in diesel particulates enhance its physiological response [50]. Carbonyl group species include HCHO, HCOOH, and HNCO, which are considered to be harmful to the human health. HCHO and HCOOH are the intermediate species formed during the combustion process and are emitted in the exhaust gas, mainly due to incomplete combustion. Literature shows that carbamylation of proteins by cyanateanions (NCO^-) is responsible for several negative health effects ranging from cardiovascular and ocular impairments, to chronic diseases such as rheumatoid arthritis [50,51].

HCHO emission was a result of partial combustion of fuel and lubricating oil in the combustion chamber. Fig. 7 showed that HCHO emission first decreased with increasing BMEP and then increased slightly at the highest BMEP. Increasing BMEP resulted in higher in-cylinder temperature, which led to more complete combustion, leading to lower HCHO emission. However, at higher BMEP, presence of richer fuel–air mixture resulted in higher degree of incomplete combustion, leading to slightly higher HCHO emission. Alcohol blending with mineral diesel resulted in a specific trend of HCHO emission. Among different diesohols, DB10 showed relatively lower HCHO emission compared to DM10 and DE10. This may be due to combined effect of higher calorific value and lower oxygen mass fraction of butanol. HCOOH emission from mineral diesel-fueled engine increased with increasing BMEP, however in diesohols, the trend was exactly reverse (Fig. 7). At lower engine loads, HCOOH emission from diesohol-fueled engine was higher compared to mineral diesel, however, at higher engine loads, mineral diesel-fueled engine emitted relatively higher HCOOH emission. Among all test fuels, DB10 emitted the lowest HCOOH, which was almost constant (~0.8 ppm) at all engine loads. With increasing BMEP, continuous reduction in HCOOH emission from

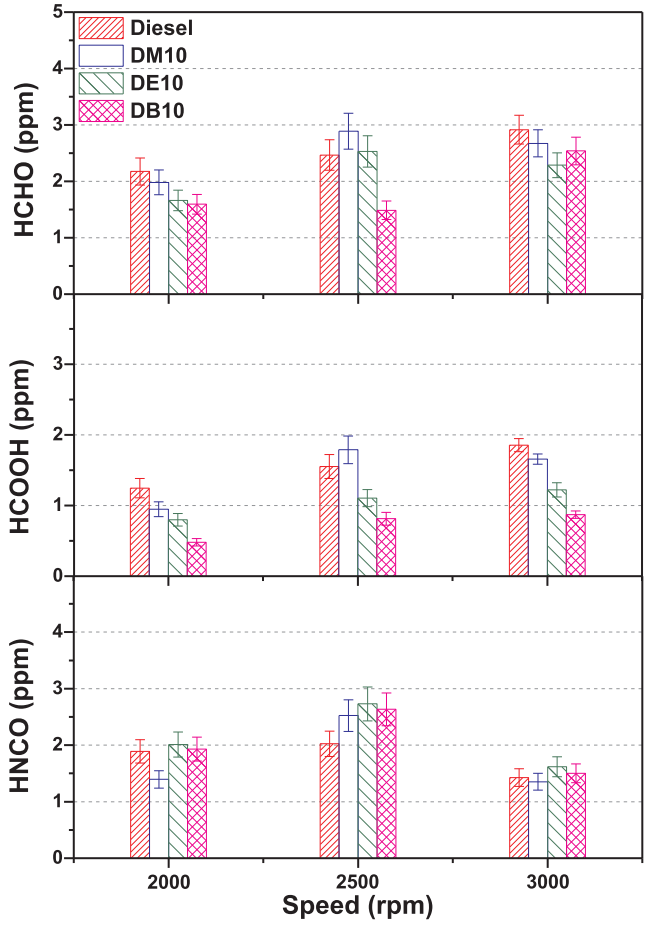

Fig. 8. Unregulated emission (carbonyl species) characteristics of diesohols with varying engine speeds at constant BMEP of 6 bar.

DM10 and DE10 was another important observation, which showed the combined effect of temperature and fuel oxygen, leading to higher degree of completion of combustion. Agarwal et al. [30] also reported similar trends of emission of carbonyl species. HNCO emission was yet another important unregulated species, which forms in higher quantities, when NO, CO, and H_2/NH_3 react in presence of precious metals [50].

Fig. 7 shows that HNCO emission for mineral diesel-fueled engine remained almost constant (~2 ppm) up to 9 bar BMEP and then decreased slightly at 12 bar BMEP. Diesohol-fueled engine showed a random pattern of HNCO emission. At low and high BMEPs, HNCO emission was slightly lower compared to mineral diesel, however at intermediate BMEPs, diesohol-fueled engine emitted relatively higher HNCO emission compared to mineral diesel. Among different diesohols, DM10 emitted the least amount of HNCO compared to DE10 and DB10.

Fig. 8 showed variations of HCHO, HCOOH and HNCO emissions at different engine speeds at constant BMEP of 6 bar. Engine speed affects the time available for completion of the combustion process hence at too high engine speed, emission of intermediate combustion products increases. Fig. 8 showed that HCHO emission increased with increasing engine speed. At medium engine speed, HCHO emission from diesohol-fueled engine was slightly higher compared to mineral diesel, however at low and high engine speeds, diesohol-fueled engine emitted relatively lower HCHO. Among different alcohols, DM10 emitted slightly higher HCHO compared to DE10 and DB10. HCOOH emission trend was similar to HCHO emission, which increased with increasing engine speed. Among different diesohols, DM10 emitted slightly higher HCOOH compared to DE10 and DB10. HNCO emission at different engine speeds showed an interesting trend. For all test fuels, HNCO

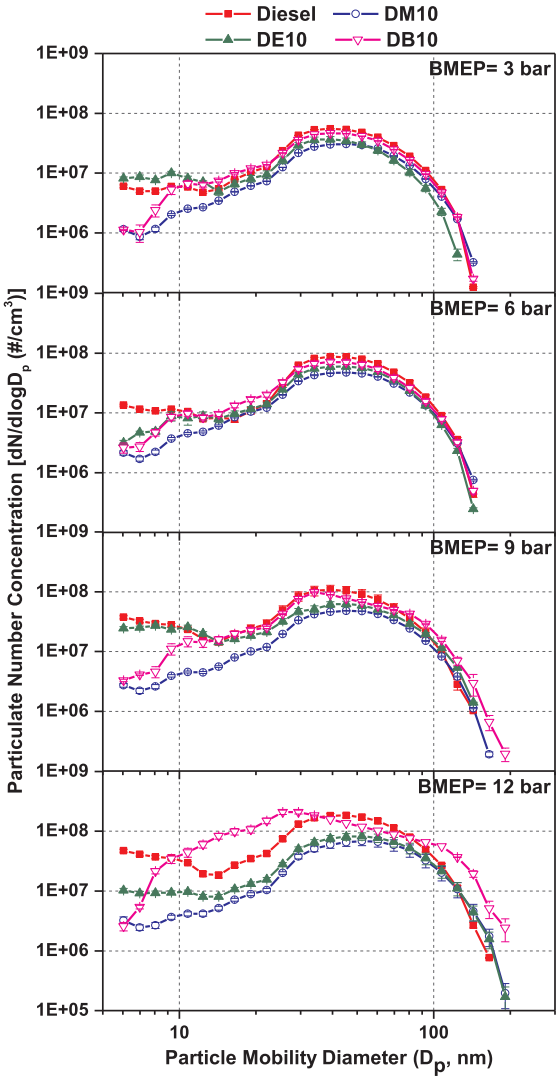

Fig. 9. Number-size distribution of particles from diesohols with varying BMEPs at constant engine speed of 2500 rpm.

emission first increased with increasing engine speed from 2000 rpm to 2500 rpm and then decreased at 3000 rpm. This was mainly due to relatively longer synthesis time required for HNCO formation. Results showed that mineral diesel-fueled engine emitted relatively lower HNCO. This might be due to higher degree of completion of combustion of mineral diesel compared to diesohols. Among different diesohols, DM10 emitted relatively lower HNCO compared to DE10 and DB10.

3.3. Particulate emissions

For exhaust particulate characterization from diesohols, exhaust gas was sampled using EEPS for one minute at a sampling frequency of 1 Hz. The average data of the 60 data sets was used for further analysis. In this study, PM characterization included particle number-size distribution, particle number-mass distribution and optimization contours of total particle numbers (TPN) and total particle mass (TPM) at varying engine loads and speeds.

Fig. 9 shows the particle number-size distribution from DM10, DE10, DB10, and mineral diesel-fueled engine at different BMEP at constant engine speed. The number-size distribution of particles can be divided into three categories namely nano-particles (NP, Dp < 10 nm), NMP (10 nm < Dp < 50 nm) and AMP (Dp > 50 nm). For all test fuels, increasing BMEP resulted in higher peak of particle number-size

distribution, which reflected a higher number concentration of particles. With increasing engine load, shifting of the peak towards larger particle sizes was another important observation, which showed that increasing BMEP resulted in formation of higher number of AMPs. This was mainly due to higher fuel quantity injected into the engine combustion chamber, resulting in longer combustion duration, therefore availability of longer time for particulate agglomeration.

For all test fuels, increasing BMEP also led to a slightly higher number of NPs, which were in different range for all test fuels. Presence of intense in-cylinder conditions may be a probable reason, which promoted pyrolysis of fuel and lubricating oil. Among different test fuels, mineral diesel exhibited greater tendency of NP emissions compared to other test fuels. This might be due to higher in-cylinder temperature and lesser availability of oxygen, which enhanced soot precursor formation, i.e. more NPs [52]. At higher BMEP, particle number-size distribution showed a significant difference in the concentration of NMPs (especially in the size range 15 to 30 nm). At all engine loads, diesohols emitted lower particle number concentrations compared to mineral diesel. The presence of oxygen in the fuel molecules is an important reason for this trend, which improved soot oxidation during post-combustion processes [53–55]. Verma et al. [52] reported that the use of oxygenated fuels resulted in soot particles having disordered nano-structure with shorter and more curved graphitic layers/fringes, which led to relatively higher soot reactivity compared to straight fringes. Superior spray characteristics of diesohols due to lower viscosity and density compared to mineral diesel may be an important factor for lower particle concentration from these test fuels [53]. Vallinayagam et al. [54] reported that lower viscosity and cetane number of oxygenated fuels improve the soot oxidation. Improved fuel spray characteristics lead to homogeneous fuel–air mixing, more complete combustion and reduction in combustion duration, which are important factors affecting particulate formation. Among different diesohols, DM10 showed the lowest particle number concentration, followed by DE10. Presence of higher oxygen content (w/w) in DM10 compared to other test fuels is the main reason for the lowest particle number concentration from DM10. Lower NPs from DM10-fueled engine at all BMEPs is another important observation, possibly due to higher latent heat of vaporization of methanol, which resulted in relatively lower in-cylinder temperature (charge cooling effect), eventually leading to lesser soot nuclei formation. With increasing BMEP, the rate of increase in particle number concentration was relatively lower for DM10 and DE10, however diesel and DB10 showed almost similar number concentration at different engine loads. This was mainly due to greater charge cooling effect of DM10 and DE10, which became dominant at higher engine loads (because of relatively higher fuel quantity injected) compared to DB10 and baseline mineral diesel [25].

Fig. 10 showed the number-size distribution of particles emitted by DM10, DE10, DB10 and mineral diesel at different BMEPs. With increasing engine speed, number concentration of particles emitted by different test fuels increased, possibly due to lesser time available for fuel-air mixing, leading to higher soot nuclei formation. At all engine speeds, diesohol-fueled engine emitted relatively lower number of particles compared to mineral diesel. Among all test fuels, DM10-fueled engine emitted lower particles compared to other diesohols (except at 2000 rpm).

Figs. 11 and 12 showed the number-mass correlation of particles emitted from diesohols and mineral diesel-fueled engine at different engine loads and speeds respectively. In this correlation, larger lobe represents higher particle emissions. Horizontal inclination of the lobe reflects relative dominance of particle numbers, and vertical inclination of the lobe reflects relative dominance of particle mass [56].

Fig. 11 showed that increasing BMEP resulted in bigger lobes of the number-mass correlation of particles, which represents that both numbers, as well as mass of particles increased with increasing BMEP. At lower engine load (3 bar BMEP), the lobes of all test fuels were symmetrical, which showed equal contribution of particle number and

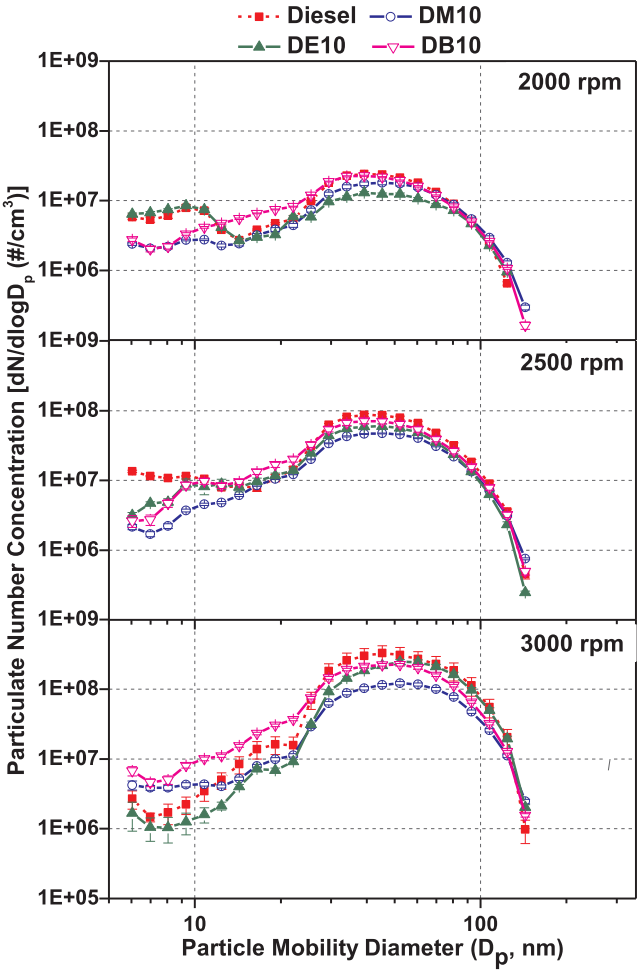

Fig. 10. Number-size distribution of particles emitted by diesohols at varying engine speeds and constant BMEP of 6 bar.

mass, however at higher BMEP, lobes were inclined towards the horizontal axis (Particle number axis). This showed that particle number concentration dominated at higher BMEPs and the contribution of smaller particles was greater in number concentration compared to larger particles. At higher BMEP, diesel lobes were inclined towards number axis more compared to diesohols, which showed that diesel-fueled engine emitted higher number particles of smaller size compared to diesohols. Similar results were reported by Agarwal et al. [25]. Among different diesohols, lobes of DM10 and DE10 were always inside the mineral diesel lobe, which showed that lower numbers as well lower mass of particles were emitted by DM10 and DE10 compared to mineral diesel. However, the lobe of DB10 showed a different pattern, especially at higher engine loads. At 12 bar BMEP, presence of two peaks in lobes of DB10 (outside of the diesel lobe) showed two extreme points for both particle numbers as well as mass dominance. The first peak of DB10 lobe corresponding to higher mass and lower number concentration of particles signified presence of higher number concentration of bigger particles (AMPs). Similarly, the second peak corresponding to lower mass and higher number concentration of particles signified presence of higher number concentration of smaller particles (NPs and NMPs).

Fig. 12 showed that increasing engine speed resulted in higher particle numbers as well as mass for all test fuels. At 3000 rpm, both the number and mass of particles were significantly higher compared to that at 2000 rpm. Fig. 12 showed that at 2000 rpm, both particle number as well as the mass were lower than higher engine speeds, however inclination of lobes towards the particle number axis reflected

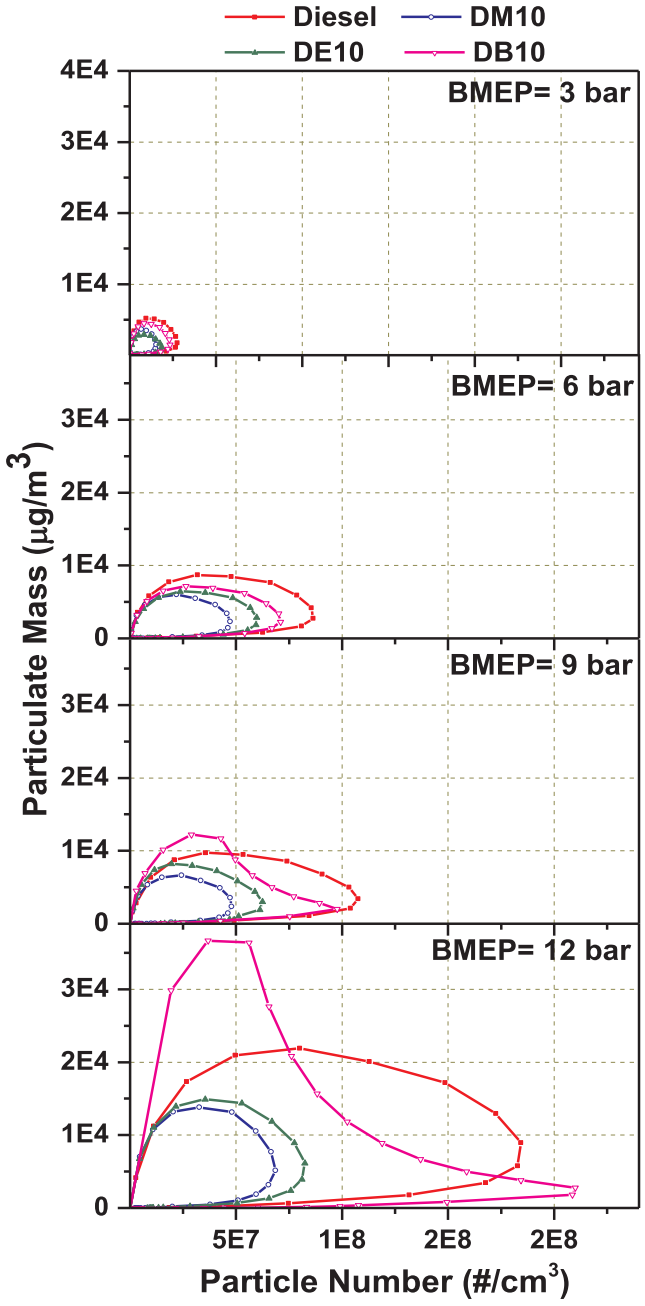

Fig. 11. Correlation between particle number and particle mass from diesohols with varying BMEPs at constant engine speed of 2500 rpm.

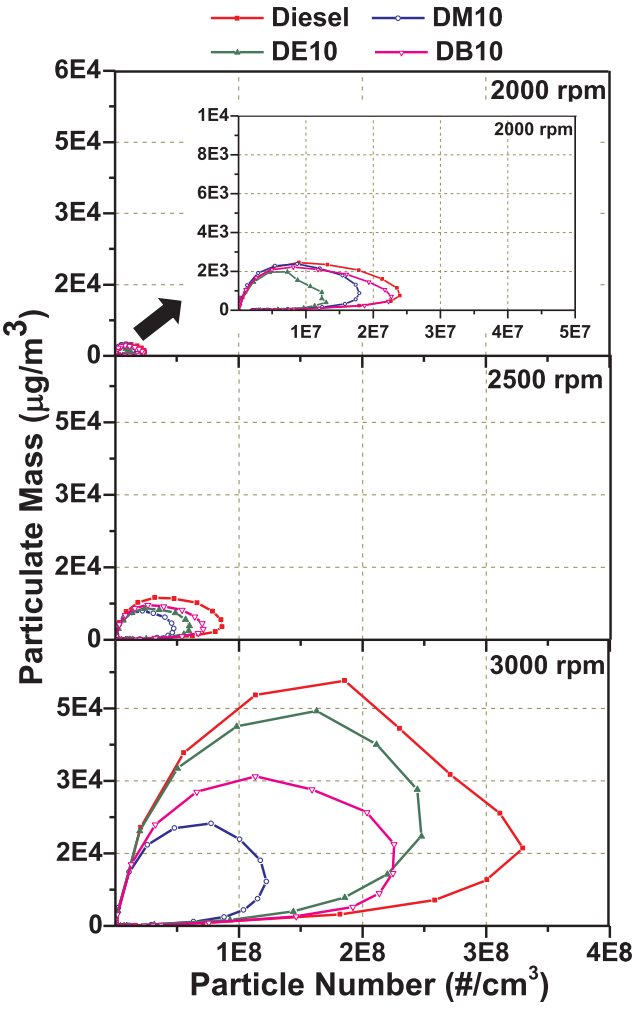

Fig. 12. Correlation between number and mass-size distribution of particles emitted by diesohols with varying engine speeds at constant BMEP of 6 bar.

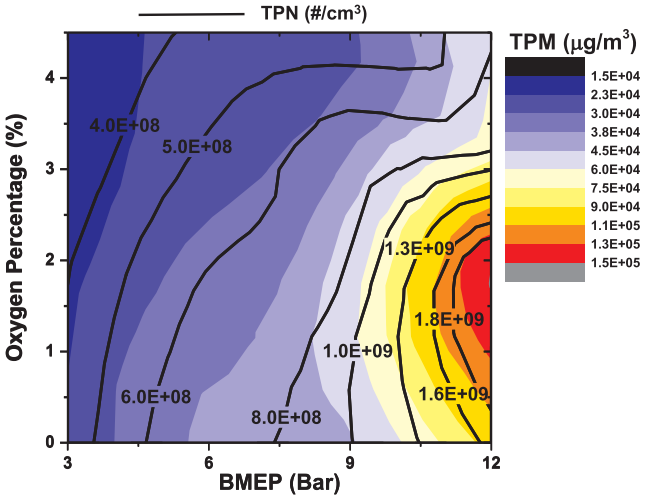

Fig. 13. Correlation between particle number and mass-size distributions from diesohols with varying BMEPs at constant engine speed of 2500 rpm.

dominance of particle numbers compared to particle mass. This was mainly due to higher time available at lower engine speeds, which in-turn provided more time for oxidation of adsorbed hydrocarbons on the particle surface. With increasing engine speed, the lobes became more symmetrical compared to lower engine speeds, which reflected equal contribution of number and mass in the particle emissions. Among different test fuels, mineral diesel showed significantly higher particle emissions (for both numbers as well as mass) compared to diesohols. This was due to presence of inherent oxygen atoms in alcohol molecules, which promoted soot oxidation, resulting in relatively lower particle numbers as well as mass. Among different alcohols, lobes of DM10 at different engine speeds (except 2000 rpm) were smaller compared to DE10 and DB10, which represented relatively lower PM emissions from DM10-fueled engine.

Figs. 13 and 14 show the TPN and TPM emitted from DM10 (~4.75% oxygen, w/w), DE10 (~3.25% oxygen, w/w), DB10 (~1.5% oxygen, w/w) and mineral diesel (No oxygen, w/w)-fueled engine at different engine loads and speeds respectively. In these figures, background color represents the TPN variations and line represents the TPM variations. These figures show the overall particulate characteristics

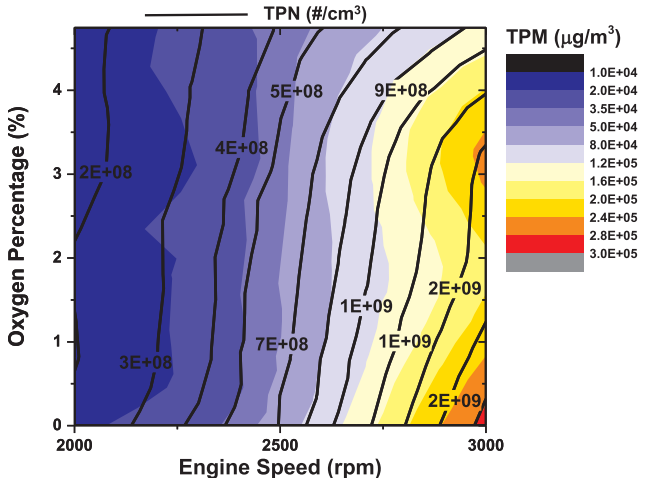

Fig. 14. Correlation between particle number and mass-size distributions from diesohols with varying engine speeds at constant BMEP of 6 bar.

(irrespective of particle size) w.r.t. oxygen content in the test fuel at varying engine speeds and loads.

Fig. 13 showed that contours of TPN and TPM variations followed a similar trend with increasing BMEP. At low-to-medium engine loads, the effect of oxygen was not significant, which resulted in higher TPN as well as TPM. However at higher engine loads, both TPN and TPM reduced with increasing oxygen content in the test fuels. This reduction was more dominant at higher oxygen containing blend (DM10), which was also visible in the particle number-size distribution. Blends with higher oxygen content exhibited almost constant TPN at higher engine loads, however TPM showed slight increase. This was due to the combined effect of two properties of methanol namely: higher fuel oxygen availability, and higher latent heat of vaporization. Presence of higher oxygen content in DM10 led to higher soot oxidation, however higher heat of vaporization resulted in lower in-cylinder temperature, therefore greater deposition of volatile species on the particle surface. This trade-off was absent in other diesohols though. These contours showed that maximum TPN ($2x10^9$ particles/cm^3 of the exhaust gas) was observed at 12 bar BMEP in ~ 0.5% to 2% fuel oxygen (w/w) region, which corresponds to DB10. Similarly, maximum TPM ($1.5x10^5$ μg/m^3 of exhaust gas) was observed at 12 bar BMEP for ~ 1% to 2% fuel oxygen (w/w) region, which also corresponds to DB10. Fig. 13 showed that DM10 has greater potential for TPN and TPM reduction, especially at higher engine loads.

Fig. 14 showed the TPN and TPM emitted from DM10, DE10, DB10 and mineral diesel-fueled engine at different engine speeds at constant BMEP of 6 bar. Results showed that contours of TPN and TPM followed a similar trend at different engine speeds. Both TPN and TPM were lower at lower engine speeds, which increased with increasing speed. Fig. 14 showed that the effect of oxygen in the test fuels was not significant up to medium engine speeds, however DM10 showed a marginal reduction in TPN and TPM at higher engine speeds. These contours showed that maximum TPN ($2x10^9$ particles/cm^3 of exhaust gas) was observed at 2500 rpm for 0% to ~ 3% fuel oxygen (w/w) region, which corresponds to mineral diesel, DB10, and DE10. Similarly, maximum TPM ($2.5x10^5$ μg/m^3 of exhaust gas) was found at 3000 rpm for 0% to ~ 0.5% fuel oxygen (w/w) region and ~ 3% to ~ 3.5% fuel oxygen (w/w) region, which corresponds to mineral diesel and DE10 respectively. Fig. 14 showed that DM10 has significant potential to reduce TPN and TPM at higher engine loads, however DB10 showed some potential of TPM reduction at higher engine speeds. Overall, Figs. 13 and 14 showed that the effect of oxygen on TPN and TPM reduction was more dominant than the one due to BMEP variations. However, engine speed variations didn't show any noticeable effect. Dominant contribution of time factor at higher engine speeds might be a main reason for this.

4. Conclusions

In this study, performance, regulated emissions, unregulated emissions, and PM emission characteristics of a medium-duty transportation CRDI engine fueled with different diesohol blends of methanol, ethanol, and butanol were compared with that of baseline mineral diesel. Results showed that alcohol blending with mineral diesel improved the BTE and reduced NOx emissions, especially at higher engine loads and speeds, where higher emissions still remained a prime concern from transport diesel engines. Unregulated emissions from different test fuels showed that diesohols emitted relatively lower NO and SO_2 compared to mineral diesel, however, HCHO, HCOOH, and HNCO emissions from diesohol-fueled engine were relatively higher compared to baseline mineral diesel. Significant reduction in particulate emissions from diesohol-fueled engine compared to mineral diesel was an important finding of this study. This reduction was dominant at extreme engine operating conditions, which was upto 60% for DM10. Particle number-mass correlations for different test fuels showed that DM10 has great potential to reduce PM emissions compared to DE10 and DB10. Overall, this study showed that blending of primary alcohols, especially methanol, with mineral diesel can improve engine performance and reduce emissions at high engine loads and speeds in modern transportation CRDI engines.

CRediT authorship contribution statement

Vikram Kumar: Writing - original draft, Investigation, Data curation. **Akhilendra Pratap Singh:** Writing - original draft, Validation, Resources, Investigation, Formal analysis. **Avinash Kumar Agarwal:** Writing - review & editing, Resources, Project administration, Investigation, Conceptualization.

Declaration of Competing Interest

The authors declare that they have no known competing financial interests or personal relationships that could have appeared to influence the work reported in this paper.

Acknowledgements

Financial support from Council for Scientific and Industrial Research (CSIR), Government of India's SRA scheme to Dr. Vikram Kumar is gratefully acknowledged, which supported his stay at ERL, IIT Kanpur for conducting these experiments.

Appendix A. Supplementary data

Supplementary data to this article can be found online at https://doi.org/10.1016/j.fuel.2020.118269.

References

[1] Maricq MM. Chemical characterization of particulate emissions from diesel engines: A review. J Aerosol Sci 2007;38(11):1079–118. https://doi.org/10.1016/j.jaerosci.2007.08.001.
[2] Jain A, Singh AP, Agarwal AK. Effect of split fuel injection and EGR on NOx and PM emission reduction in a low temperature combustion (LTC) mode diesel engine. Energy 2017;122:249–64.
[3] Heywood JB. Internal combustion engine fundamentals. New York: McGraw-Hill Book Company; 1988.
[4] Zhu M, Setyawan HY, Zhang Z, Zhang D. Effect of n-butanol addition on the burning rate and soot characteristics during combustion of single droplets of diesel–biodiesel blends. Fuel 2020;265:117020.
[5] Chen H, Su X, He J, Xie B. Investigation on combustion and emission characteristics of a common rail diesel engine fueled with diesel/n-pentanol/methanol blends. Energy 2019;167:297–311.
[6] Li G, Lee TH, Liu Z, Lee CF, Zhang C. Effects of injection strategies on combustion

and emission characteristics of a common-rail diesel engine fueled with iso-propanol-butanol-ethanol and diesel blends. Renewable Energy 2019;130:677–86.
[7] Emiroğlu AO. Effect of fuel injection pressure on the characteristics of single cylinder diesel engine powered by butanol-diesel blend. Fuel 2019;256:115928.
[8] Verhelst S, Turner JW, Sileghem L, Vancoillie J. Methanol as a fuel for internal combustion engines. Prog Energy Combust Sci 2019;70:43–88.
[9] Çelebi Y, Aydın H. An overview on the light alcohol fuels in diesel engines. Fuel 2019;236:890–911.
[10] Agarwal AK. Biofuels (alcohols and biodiesel) applications as fuels in internal combustion engines. Prog Energy Combust Sci 2007;32:233–71. https://doi.org/10.1016/j.pecs.2006.08.003.
[11] Emiroğlu AO, Şen M. Combustion, performance and emission characteristics of various alcohol blends in a single cylinder diesel engine. Fuel 2018;212:34–40.
[12] Li S, Liu J, Wang F, Li Y, Wei M, Xiao H, et al. Effects of gasoline and iso-butanol addition on combustion and pollutant emissions of a common-rail diesel engine at different injection timing. Fuel 2019;256:115853.
[13] Luo J, Zhang Y, Wang J, Zhang Q. Effect of acetone–butanol– ethanol addition to diesel on the soot reactivity. Fuel 2018;226:555–63.
[14] Rakopoulos CD, Rakopoulos DC, Kosmadakis GM, Papagiannakis RG. Experimental comparative assessment of butanol or ethanol diesel-fuel extenders impact on combustion features, cyclic irregularity, and regulated emissions balance in heavy-duty diesel engine. Energy 2019;174:1145–57.
[15] Sirignano M, Ciajolo A, D'Anna A, Russo C. Chemical features of particles generated in an ethylene/ethanol premixed flame. Energy Fuels 2017;31(3):2370–7.
[16] Guan C, Cheung CS, Li X, Huang Z. Effects of oxygenated fuels on the particle-phase compounds emitted from a diesel engine. Atmos Pollut Res 2017;8(2):209–20.
[17] Li Z, Wang Y, Geng H, Zhen X, Liu M, Xu S, et al. Effects of diesel and methanol injection timing on combustion, performance, and emissions of a diesel engine fueled with directly injected methanol and pilot diesel. Appl Therm Eng 2019;163:114234.
[18] Ghadikolaei MA, Wei L, Cheung CS, Yung KF, Ning Z. Particulate emission and physical properties of particulate matter emitted from a diesel engine fueled with ternary fuel (diesel-biodiesel-ethanol) in blended and fumigation modes. Fuel 2020;263:116665.
[19] Chen C, Yao A, Yao C, Wang B, Lu H, Feng J, et al. Study of the characteristics of PM and the correlation of soot and smoke opacity on the diesel methanol dual fuel engine. Appl Therm Eng 2019;148:391–403.
[20] Lapuerta M, Armas O, García-Contreras R. Effect of ethanol on blending stability and diesel engine emissions. Energy Fuels 2009;23(9):4343–54.
[21] Cheung CS, Zhang ZH, Chan TL, Yao C. Investigation on the effect of port-injected methanol on the performance and emissions of a diesel engine at different engine speeds. Energy Fuels 2009;23(11):5684–94. https://doi.org/10.1021/ef9005516.
[22] Jiotode Y, Agarwal AK. Endoscopic combustion visualization for spatial distribution of soot and flame temperature in a diesohol fueled compression ignition engine. Energy Fuels 2016;30(11):9850–8. https://doi.org/10.1021/acs.energyfuels.6b01585.
[23] Satsangi DP, Tiwari N. Experimental investigation on combustion, noise, vibrations, performance and emissions characteristics of diesel/n-butanol blends driven genset engine. Fuel 2018;221:44–60.
[24] Jin C, Pang X, Zhang X, Wu S, Ma M, Xiang Y, et al. Effects of C3–C5 alcohols on solubility of alcohols/diesel blends. Fuel 2019;236:65–74.
[25] Agarwal AK, Sharma N, Singh AP, Kumar V, Satsangi DP, Patel C. Adaptation of methanol-dodecanol-diesel blend in diesel genset engine. J Energy Res Technol 2019;141:102203–11. https://doi.org/10.1115/1.4043390.
[26] Ning L, Duan Q, Chen Z, Kou H, Liu B, Yang B, et al. A comparative study on the combustion and emissions of a non-road common rail diesel engine fueled with primary alcohol fuels (methanol, ethanol, and n-butanol)/diesel dual fuel. Fuel 2020;266:117034.
[27] Wu Y, Zhang X, Zhang Z, Wang X, Geng Z, Jin C, et al. Effects of diesel-ethanol-THF blend fuel on the performance and exhaust emissions on a heavy-duty diesel engine. Fuel 2020;271:117633.
[28] Canakci M, Sayin C, Ozsezen AN, Turkcan A. Effect of injection pressure on the combustion, performance, and emission characteristics of a diesel engine fueled with methanol-blended diesel fuel. Energy Fuels 2009;23:2908–20. https://doi.org/10.1021/ef900060s.
[29] Huang Z, Lu H, Jiang D, Zeng KJ, Liu J, Liu B, et al. Engine performance and emissions of a CI engine operating on the diesel-methanol blends. Proc Inst Mech Eng, Part D: J Automobile Eng 2004;218:435–47. https://doi.org/10.1243/095440704773599944.
[30] Agarwal AK, Shukla PC, Patel C, Gupta JG, et al. Unregulated emissions and health risk potential from biodiesel (KB5, KB20) and methanol blend (M5) fueled transportation diesel engines. Renewable Energy 2016;98:283–91. https://doi.org/10.1016/j.renene.2016.03.058.
[31] Zhou D, Qiu C. Experimental Study on Unregulated Emissions Characteristics of Alcohol-Diesel Dual-Fuel Combustion with Diesel Oxidation Catalyst. J. Energy Eng 2019;145(2):04018075. https://doi.org/10.1061/(ASCE) EY.1943-7897.0000596.
[32] Fan C, Song C, Lv G, Wang G, Zhou H, Jing X. Evaluation of carbonyl compound emissions from a non-road machinery diesel engine fueled with a methanol/diesel blend. Appl Therm Eng 2018;129:1382–91.
[33] Sayin C. Engine performance and exhaust gas emissions of methanol and ethanol–diesel blends. Fuel 2010;89:3410–5. https://doi.org/10.1016/j.fuel.2010.02.017.
[34] Jamrozik A. The effect of the alcohol content in the fuel mixture on the performance and emissions of a direct injection diesel engine fueled with diesel-methanol and diesel-ethanol blends. Energy Convers Manage 2017;148:461–76. https://doi.org/10.1016/j.enconman.2017.06.030.
[35] Merritt PM, Ulmet V, McCormick RL, Mitchell WE, Baumgard KJ. Regulated and unregulated exhaust emissions comparison for three tier II non-road diesel engines operating on ethanol-diesel blends. SAE transactions 2005; 2005-1111-1122.
[36] He BQ, Shuai SJ, Wang JX, He H. The effect of ethanol blended diesel fuels on emissions from a diesel engine. Atmos Environ 2003;37(35):4965–71. https://doi.org/10.1016/j.atmosenv.2003.08.029.
[37] Cheung CS, Di Y, Huang Z. Experimental investigation of regulated and unregulated emissions from a diesel engine fueled with ultralow-sulfur diesel fuel blended with ethanol and dodecanol. Atmos Environ 2008;42(39):8843–51. https://doi.org/10.1016/j.atmosenv.2008.09.009.
[38] Lapuerta M, Hernández JJ, Rodríguez-Fernández J, Barba J, Ramos A, Fernández-Rodríguez D. Emission benefits from the use of n-butanol blends in a Euro 6 diesel engine. Int J Engine Res 2018;19(10):1099–112. https://doi.org/10.1177/1468087417742578.
[39] Chen Z, Liu J, Han Z, Du B, Liu Y, Lee C. Study on performance and emissions of a passenger-car diesel engine fueled with butanol–diesel blends. Energy 2013;55:638–46. https://doi.org/10.1016/j.energy.2013.03.054.
[40] Choi B, Jiang X, Kim YK, Jung G, Lee C, Choi I, et al. Effect of diesel fuel blend with n-butanol on the emission of a turbocharged common rail direct injection diesel engine. Appl Energy 2015;146:20–8. https://doi.org/10.1016/j.apenergy.2015.02.061.
[41] Yusri IM, Mamat R, Akasyah MK, Jamlos MF, Yusop AF. Evaluation of engine combustion and exhaust emissions characteristics using diesel/butanol blended fuel. Appl Therm Eng 2019;156:209–19. https://doi.org/10.1016/j.applthermaleng.2019.02.028.
[42] Kim KH, Choi B, Park S, Kim E, Chiaramonti D. Emission characteristics of compression ignition (CI) engine using diesel blended with hydrated butanol. Fuel 2019;257:116037.
[43] Liu B, Cheng X, Liu J, Pu H. Investigation into particle emission characteristics of partially premixed combustion fueled with high n-butanol-diesel ratio blends. Fuel 2018;223:1–11.
[44] Singh AP, Bajpai N, Agarwal AK. Combustion mode switching characteristics of a medium-duty engine operated in compression ignition/PCCI combustion modes. J Energy Resour Technol, Transactions of the ASME 2018;140(9):092201https://doi.org/10.1115/1.4039741.
[45] Singh AP, Pal A, Agarwal AK. Comparative particulate characteristics of hydrogen, CNG, HCNG, gasoline and diesel fueled engines. Fuel 2016;185:491–9. https://doi.org/10.1016/j.fuel.2016.08.018.
[46] A.P. Singh N. Sharma V. Kumar D.P. Satsangi A.K. Agarwal Fuel Injection Strategy for Utilization of Mineral Diesel-Methanol Blend in a Common Rail Direct Injection Engine Journal of Energy Resources Technology 2020 142(8).
[47] Indian standard IS: 14273, Automotive vehicles – Exhaust emissions – Gaseous pollutants from vehicles fitted with compression ignition engines – method of measurement, Bureau of Indian Standards 1999 New Delhi India.
[48] Lee S, Lee CS, Park S, Gupta JG, Maurya RK, Agarwal AK. Spray characteristics, engine performance and emissions analysis for Karanja biodiesel and its blends. Energy 2017;119:138–51.
[49] Pan S, Li X, Han W, Huang Y. An experimental investigation on multi-cylinder RCCI engine fueled with 2-butanol/diesel. Energy Convers Manage 2017;154:92–101. https://doi.org/10.1016/j.enconman.2017.10.047.
[50] Brady JM, Crisp TA, Collier S, Kuwayama T, Forestieri SD, Perraud V, et al. Real-time emission factor measurements of isocyanic acid from light duty gasoline vehicles. Environ. Sci. Technol. 2014;48:11405–12. https://doi.org/10.1021/es504354p.
[51] Singh AP, Agarwal AK. Partially homogenous charge compression ignition engine development for low volatility fuels. Energy Fuels 2017;31(3):3164–81. https://doi.org/10.1021/acs.energyfuels.6b02832.
[52] Verma P, Jafari M, Rahman SMA, Pickering E, Stevanovi S, Dowell A, et al. The impact of chemical composition of oxygenated fuels on morphology and nanostructure of soot particles. Fuel 2020;2591:116167.
[53] Hwang J, Jung Y, Bae C. Particulate morphology of waste cooking oil biodiesel and diesel in a heavy duty diesel engine. Int Conf Opt Part Charact 2014;9232:1–6.
[54] Vallinayagam R, Vedharaj S, Yang WM, Roberts WL, Dibble RW. Feasibility of using less viscous and lower cetane (LVLC) fuels in a diesel engine: a review Renew Sustain. Energy Rev 2015;51:1166–90.
[55] A.P. Singh A.K. Agarwal CI/PCCI combustion mode switching of diesohol fueled production engine SAE Technical Paper 2017; 2017–01-0738. 10.4271/2017-01-0738.
[56] Shukla PC, Gupta T, Gupta NK, Agarwal AK. A qualitative correlation between engine exhaust particulate number and mass emissions. Fuel 2017;202:241–5. https://doi.org/10.1016/j.fuel.2017.04.016.